Int. J. Solids Structures Vol. 14, pp. 639–653

0020-7683/78/0801-0639/$02.00/0

DYNAMIC PROPAGATION AND ARREST MEASUREMENTS BY THE METHOD OF CAUSTICS ON OVERLAPPING SKEW-PARALLEL CRACKS

P. S. THEOCARIS

Department of Theoretical and Applied Mechanics, The National Technical University, Athens 625, Greece

(*Received* 16 *August* 1977; *in revised form* 27 *December* 1977; *received for publication* 1 *February* 1978)

Abstract—In this paper the quasi-static and dynamic behaviour of two skew-parallel and unequal edge cracks in a brittle material, namely PMMA, was investigated. The study was undertaken by using the optical method of caustics in combination with a high-speed Cranz–Schardin camera for recording the various steps of the statically or the dynamically propagated cracks. From the whole study it was deduced that, for the case of the quasi-static loading and for all geometrical configurations of cracks, only the longer crack was propagated, while the shorter crack remained stationary. The propagation path of the longer crack curved towards the opposite edge crack. Both edge cracks propagated simultaneously only under the dynamic loading mode and under certain favourable combinations of the geometrical configurations of the cracked specimen. Both edge cracks curved, under quasi-static loading and strong tendency for crack arrest phenomena was observed. The values of the crack propagation velocity and the stress intensity factors for both cracks were determined and were found to be larger for the dynamic than for the quasi-static loading case.

INTRODUCTION

The significance in engineering applications of crack propagation phenomena in brittle materials has led many researchers to the investigation of these phenomena. A great number of papers[1, 2] has appeared in the literature, studying the fracture process in brittle materials under dynamic loading, either theoretically or experimentally. High crack propagation velocities of the order of 60% of the velocity of the respective Rayleigh wave, which is an upper limit in crack propagation velocities[3], have also been observed.

Existing theoretical solutions of crack propagation phenomena are based either on energy methods or on dynamic elasticity. Some of them express the crack velocity as a function of material properties, while others investigate the dynamic stress field surrounding the running crack. Experimentally, the problem has been usually attacked with the method of high speed photography in conjunction with the existing methods of experimental stress analysis, like photoelasticity, moiré, holography and caustics. The method of high speed photography has the advantage over the methods based on ultrasonics and velocity gauges that it can provide information not only about the crack propagation velocity, as the latter methods do, but also about the stress field at the tip of the running crack, when combined with some other method of experimental stress analysis. A concise survey on the existing literature on crack propagation phenomena is given in Ref. [4].

Regarding the particular problem of the mechanism of crack propagation in brittle and semi-brittle materials, Theocaris and Katsamanis have already studied in a previous paper[4] crack propagation phenomena under impact loading by using the optical method of caustics in combination with a Cranz–Schardin high speed camera. They found that the crack is propagated only under the influence of the tensile part of the loading pulse, whereas the crack remains stationary when it is loaded by the compressive part of the pulse. Thus, when a stress pulse is applied to a cracked specimen and it is reflected from the transverse edges of the specimen, the crack is propagated in a stepwise manner, only in time intervals when the tensile parts of the pulse are operative. It was also found in Ref.[4] that the maximum crack propagation velocity, as well as the intervals at which the crack is propagated under each pulse depend on the amplitude of the corresponding pulse and the initial crack length. However, this experimental study was concerned with the phenomenon of propagation of a single crack in a brittle material which does not contain any other discontinuity and it was devoted to evaluating the crack propagation velocity under various loading conditions and as a function of the material properties, as well as the instantaneous crack tip stress intensity factors.

In practice, the case when existing cracks in a plate interact with other discontinuities is very common. Many attempts have been made to study the crack propagation characteristics in brittle materials in which there exist other discontinuities also. Thus, Kobayashi *et al.*[5] studied the interaction of a central hole and a propagating crack in Homalite by using dynamic photoelasticity in combination with a high-speed camera. They observed crack arrest phenomena and compared the elasto-dynamic state of stress with the corresponding elastostatic state of the same problem, which was determined by a finite-element analysis.

Ishikawa *et al.*[6] studied the behaviour of a rapidly moving crack around a small hole in PMMA and determined the variation of the stress intensity factor, as well as the crack velocity, at various stages of crack propagation. Contrary to the results by Kobayashi *et al.*[5], they found that the crack velocity is larger when the crack recedes from the vicinity of the hole than when the crack is approaching the hole. Also they determined the time interval of the crack arrest during its passage from the hole and they found that this interval increases with the diameter of the hole while it diminishes as the fracture stress of the material of the specimen is reduced.

On the other hand, a great number of papers has been devoted to the interaction of two stationary cracks. Thus, Barenblatt[7] gave a summary of papers dealing with elastic cracks. Smith[8] studied the relative displacements of the crack tips for an array of coplanar cracks under antiplane and plane-strain conditions. A similar study of the interaction of various types of cracks was presented by Yokobori *et al.*[9]. They studied the influence of the intercrack distance, related to the corresponding width of the neighbouring cracks, and the distance between successive crack tips.

More recently, Theocaris in a series of papers[10–12], studied by the optical method of caustics the interaction between two collinear and symmetric or asymmetric cracks, as well as the interaction of cracks and unloaded boundaries. He determined the crack tip stress-intensity factors and compared them with their corresponding values for a single crack. From all these studies it was concluded that there is an insignificant interaction between two collinear cracks or a crack and a straight boundary when the inside distance between the tips of the collinear cracks or the distance between the tip of a single crack and the boundary is greater than the length of the crack. However, as this distance is shortened, there is a continuous increase in the interaction between the cracks. Also, Theocaris[12] concluded that for a minimum distance between the tips of the two collinear cracks or the tip of a single crack and a straight boundary, equal to 0.25 the length of the crack, the values of the corresponding stress intensity factors are independent of the type of the discontinuity to which the crack is approaching.

Gupta and Erdogan[13] studied theoretically the plane elastostatic problem of an infinite strip containing two symmetrically located internal cracks perpendicular to the boundary. The solution of the problem was obtained for various crack geometries when the strip was subjected to uniaxial tension applied far away from the crack region.

From the above brief review it is concluded that, although a great number of papers has appeared in the literature for the study of the interaction of stationary cracks, the extent of studies of the case of statically or dynamically propagating cracks is rather limited. The purpose of the present paper is to study the phenomena related to the interaction of two overlapping skew-parallel and unequal edge cracks in PMMA, which are propagated either statically or dynamically. The optical method of caustics in combination with a Cranz–Schardin high-speed camera was used. Interesting results for the crack propagation velocities and the crack tip stress-intensity factors for both overlapping skew-parallel cracks are disclosed.

DETERMINATION OF K_I-STRESS INTENSITY FACTORS BY THE METHOD OF CAUSTICS

The stress intensity factors, characterizing the stress field in the vicinity of a crack tip for a stationary or a moving crack, were evaluated by using the optical method of caustics[14]. According to this method, a light beam is impinged on the specimen in the close vicinity of the crack tip and the transmitted rays are received on a reference plane, parallel to the plane of the specimen. These rays are scattered because of the strong thickness and refractive index variations in the region close to the crack tip and they are concentrated along a strongly illuminated curve on the reference plane (caustic).

The governing equations of the caustics on the reference plane were already found previously[10–12] and they are expressed by:

$$x' = \lambda r_0\left(\cos\vartheta + \frac{2}{3}\cos\frac{3\vartheta}{2}\right)$$
$$y' = \lambda r_0\left(\sin\vartheta + \frac{2}{3}\sin\frac{3\vartheta}{2}\right) \tag{1}$$

with:

$$r_0 = \left(\frac{3C}{2\lambda}\right)^{2/5}, \quad C = \frac{z_0 t c_t K_I}{\sqrt{2\pi}}, \quad \lambda = \frac{z_i}{z_i + z_0}. \tag{2}$$

In these relations z_0 represents the distance between the specimen and the reference plane (Fig. 1), t is the thickness of the specimen, c_t is the stress-optical coefficient for transmitted light rays and z_i denotes the distance between the plane of the specimen and the focus of each light beam.

From eqn (1) and by inserting the value $x' = 0$ (the origin of x', y' coordinate system is at the tip of the crack with the positive x'-direction along the crack direction[10–12]), it can be concluded that the transverse diameter $D_{t\lambda}(D_{t\lambda} = 2y')$ of the caustic is related to the radius r_0 of the *initial curve* of the caustic (that is the generatrix curve on the specimen, which creates the caustic on the reference screen) by the following simple relation (for PMMA):

$$D_{t\lambda} = 3.16\lambda r_0. \tag{3}$$

By substituting into this relation the value of r_0 given by relations (2), it is concluded that the stress intensity factor K_I is given by:

$$K_I = \frac{1.671}{z_0 t c_t}\frac{1}{\lambda^{3/2}}\left(\frac{D_{t\lambda}}{3.16}\right)^{5/2} \tag{4}$$

It can finally be mentioned that the foregoing formulas were derived by taking into account only the singular part of the stress field near a crack tip. In this way the use of these formulas introduces some errors in the results obtained. Nevertheless, this error is not considerable in most cases. This is due to the fact that the initial curves of the caustics on the specimen itself, which create the caustics on the reference plane, are generally very small and lie in the very close vicinity of the crack tip. Indeed, the maximum radii of the initial curves did not exceed in all cases the values of $r_0 = 1$ to 2 mm and this reduced considerably the critical length of the crack influencing the shape and size of the caustic.

On the other hand, the fact that, if the constant part of the stress field near the crack tip is taken into account, this does not have any influence on the shape of the initial curve of the

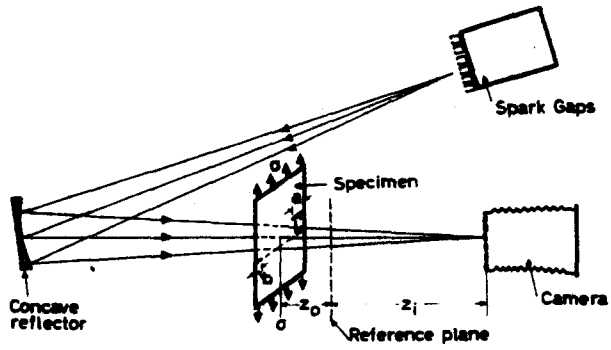

Fig. 1. Optical part of the experimental arrangement.

caustic formed near the crack tip and the caustic itself, and therefore reduces considerably the error introduced by the influence of neighboring boundaries and the curvatures of the crack axis.

These facts are contrary to what happens in the case of photoelastic or interferometric determination of stress intensity factors. In this way, it is believed that in the majority of experiments made, the results of which are given in the sequel, the values of the stress intensity factors determined by the method of caustics by using eqn (4), are good approximations of their true values.

EXPERIMENTAL ARRANGEMENT

For the experimental investigation of the behaviour of the two overlapping cracks under quasi-static and dynamic loading in a brittle material, PMMA tension specimens of thickness $t = 2.5$ mm and dimensions $300 \times 100\,\text{mm}^2$ were used. The specimens had initially two skew-parallel edge cracks of lengths a and b with a distance l between them (Fig. 1). The length a of the longer crack was taken constant and equal to $a = 23$ mm, while the length b of the shorter crack varied between 10 and 20 mm. The intercrack distance l also varied between 10 and 40 mm.

Next, the specimens were subjected either to a quasi-static or to a dynamic tensile stress until fracture, imposed by means of either a static loading tester (Fig. 2), or a falling weight set-up respectively. The stress-rate for the quasi-static load was equal to $5\,\text{kp cm}^{-2}\,\text{sec}^{-1}$, while the stress rate for the dynamic load was $8 \times 10^3\,\text{kp cm}^{-2}\,\text{sec}^{-1}$. In both cases the load was detected by means of a piezoelectric transducer connected with an oscillograph. Figure 3 presents the mode of fracture of two specimens with the same geometrical configuration ($a = 23$ mm, $b = 20$ mm, $l = 30$ mm). In the first of these tests (case (a)) the specimen was subjected to a quasi-static loading (c), while in the second test (b) the specimen was subjected to a dynamic load (d). The fracture load for the quasi-static case was equal to $P = 125$ kp, while for the dynamic-load case it was equal to $P = 155$ kp.

For the study of the fracture behaviour of the cracked specimens the optical method of caustics, in combination with a high-speed Cranz–Schardin camera, was used. This camera is composed of 24 spark-gap light sources, which can operate with any desired frequency, lower than 10^6 frames per sec. Also this camera has a suitable programmer, by means of which the frequency of the operation of its 24 light-sources can be adjusted to vary for different groups of the light-sources in accordance with any preassigned rate of sequence of its sparks. Thus, it was possible to have different frequencies of the light-sparks at different steps of the propagation of cracks and thus to record in a complete and satisfactory manner the whole phenomenon of crack propagation in the plate. The appropriate synchronization of the crack propagation process and the operation of the high-speed camera was achieved by means of an electric circuit, which was triggered as the crack started to propagate. A block diagram of the experimental set-up is shown in Fig. 2.

The optical part of the experimental arrangement is shown in Fig. 1. A light beam was

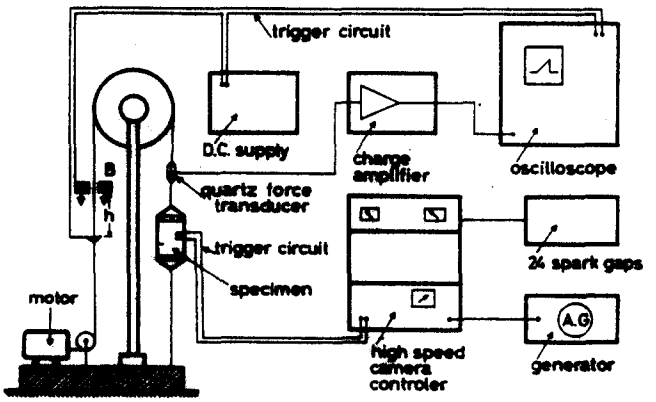

Fig. 2. Block diagram of the experimental set-up.

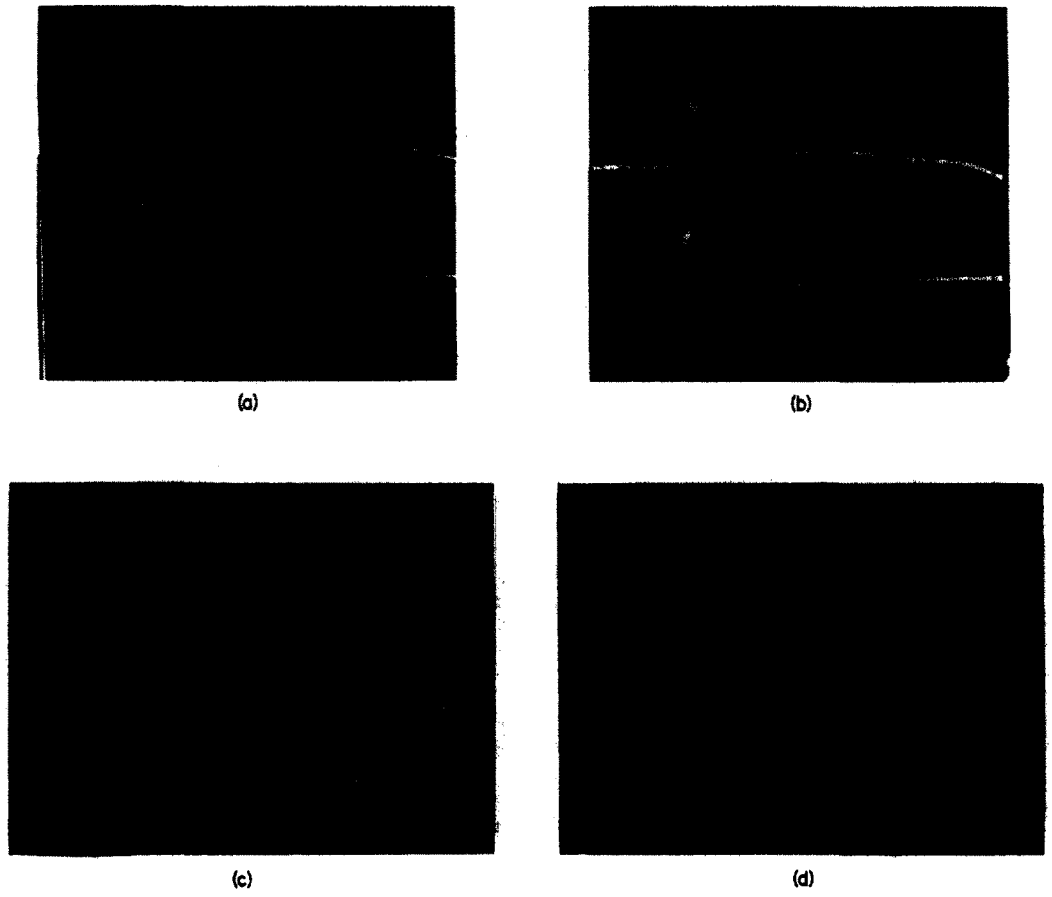

Fig. 3. Photographs of specimens showing the crack propagation paths for a static (a) and a dynamic (b) loading with their corresponding oscillograms of the load variation (c, d).

emitted from each spark and reflected from a spherical mirror of diameter equal to 50 cm and of a focal distance equal to 350 cm. The mirror could rotate about its horizontal and vertical axes by means of micrometer screws so that the reflected light beam, after passing through the specimen, could be focussed on each of the twenty-four lenses of the high-speed camera. Thus, by a suitable adjustment of the frequency of the high-speed camera twenty-four subsequent pictures can be obtained during the period of each test. A TRI-X-PAN sensitive film was used for recording the pulse patterns on each specimen during the crack propagation.

EXPERIMENTAL RESULTS

Two series of cracked specimens with two overlapping cracks, the length of one of which was constant and equal to $a = 23$ mm, the length of the other varied between 10 and 20 mm and the normal distance l between the cracks was variable, (Fig. 1) were made. The first series was loaded quasi-statically, while the second series was loaded dynamically by the respective stress rates already mentioned. Figure 4 shows a sequence of twelve photographs corresponding to a quasi-static loading of the specimen with $a = 23$ mm, $b = 20$ mm and $l = 10$ mm. At the tips of both cracks caustics are formed, which can be used for the accurate estimation of the current crack length at each time instant. Moreover, the caustics, by their size, enable the determination of the stress intensity factors. From Fig. 4 it can be observed that only the longer crack is propagated, while the shorter crack remains stationary. It can also be remarked that the propagating crack is changing direction, diverting toward the stationary crack as it is approaching this crack and overlapping it.

From a whole series of similar experiments it was concluded that for the quasi-static loading mode only the crack with the larger length was propagated. Also, at the end of the propagating crack a large amount of inelastic deformation was observed (see the last photograph of Fig. 4), which remained for a long time after the complete fracture of the specimen.

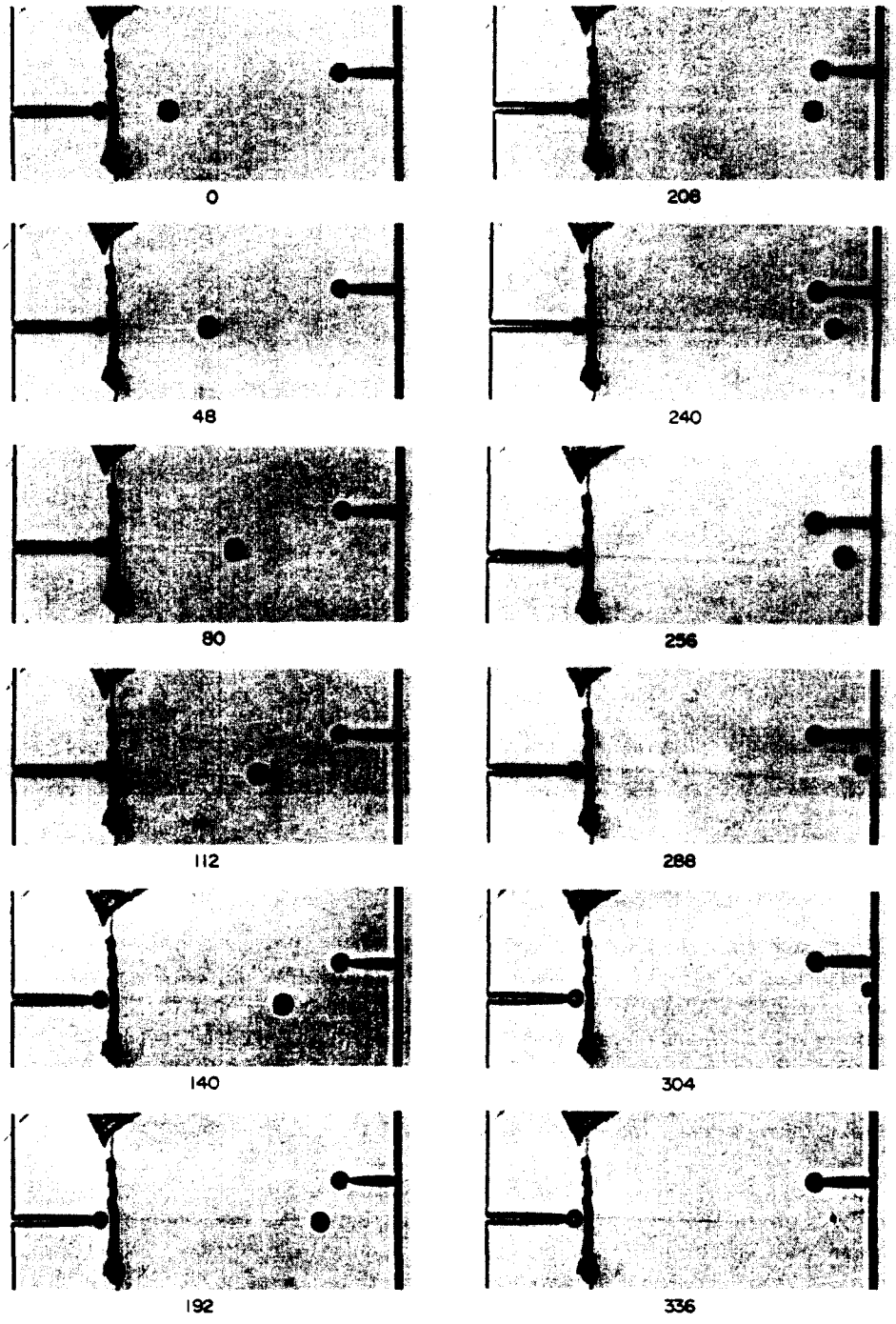

Fig. 4. Series of photographs obtained with a high-speed camera in a plexiglas specimen containing two skew-parallel edge cracks with $a = 23$ mm, $b = 20$ mm, $l = 10$ mm and subjected to a quasi-static loading up to fracture (time in μsec).

Several specimens similar to those which were loaded quasi-statically were afterwards subjected to a dynamic loading under a stress rate equal to 8×10^3 kp cm^{-2} sec^{-1}. The experimental results of the dynamic loading mode can be divided into two main categories, depending on the configuration of the cracked specimen. All specimens in which only the longer crack is propagated belong to the first category, while all specimens in which the shorter crack is also propagated sometime during the spreading of the longer crack belong to the second category. Figure 5 shows a sequence of twelve photographs corresponding to a dynamic loading to a specimen similar to the one of Fig. 4. From this figure it is observed that, contrary to the quasi-static loading mode, both cracks are propagated. An inspection of Fig. 5 shows that the

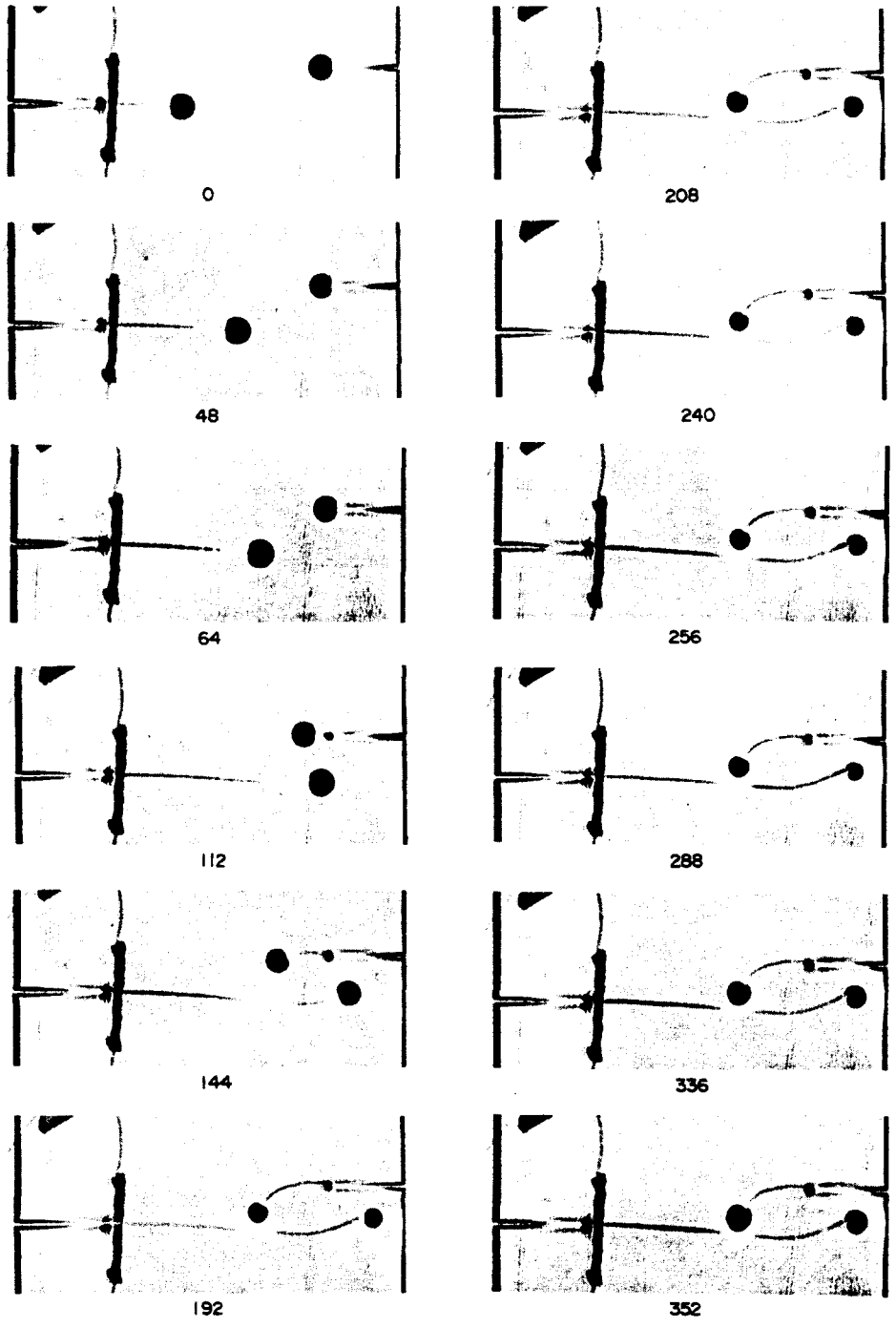

Fig. 5. Series of photographs obtained with high-speed camera in the specimen of Fig. 4 subjected to dynamic loading up to fracture (time in μsec).

longer crack is propagated first and that, as this crack approaches and overlaps the shorter crack, a strong interaction between the cracks takes plane. At this stage the shorter crack starts to propagate, while the propagation paths of both cracks are deviated from their transverse paths and curved, aiming the one toward the other.

From the photographs of Figs. 4 and 5 the variations of the actual crack lengths L_a and L_b for both edge cracks and for the quasi-static, as well as for the dynamic loading modes, were calculated and plotted in Fig. 6 vs time t. From these plottings the crack propagation velocities v_a and v_b were calculated as the derivatives of the curves $L_{a,b} = f(t)$. Figure 7 presents the variation of the crack propagation velocity v_a vs the actual crack length L_a for the quasi-static,

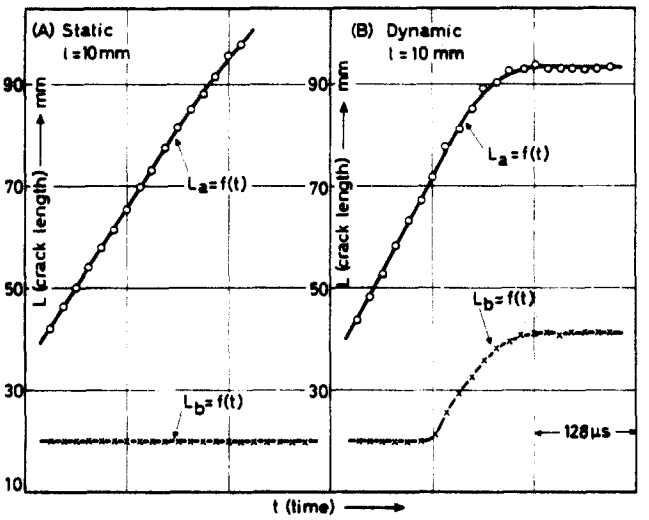

Fig. 6. Variation of the actual crack lengths L_a and L_b vs time t for the specimen of Fig. 4 subjected to quasi-static (A) or to dynamic (B) loading.

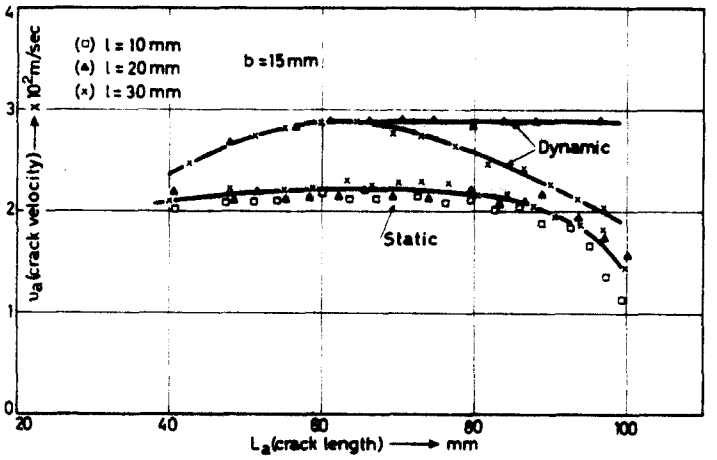

Fig. 7. Variation of the crack propagation velocity v_a of the larger crack in a doubly-cracked specimen vs the actual crack length L_a for a quasi-static and a dynamic loading which do not cause a propagation of the smaller crack.

as well as the dynamic loading modes, for constant lengths of both cracks $a = 23$ mm, $b = 15$ mm, and for an intercrack distance l equal to $l = 10$, 20 and 30 mm. The configurations of cracks in this series of specimens were such that for the dynamic loads applied to the cracked specimens only the longer crack was propagating. From Fig. 7 it is concluded that the crack propagation velocity v_a is independent of the intercrack distance l for the quasi-static loading mode, while for the dynamic loading mode the velocity v_a is strongly influenced by this distance l. Thus, for long cracks with lengths higher than $L_a = 70$ mm and for $l > 30$ mm the crack velocity v_a is highly reduced. From Fig. 7 it is also concluded that the crack propagation velocity is larger for the dynamic loading mode than the corresponding quasi-static loading mode.

Figures 8 and 9 present the variation of the crack propagation velocities v_a and v_b for the dynamic loading mode and for configurations of cracks for which both edge cracks can propagate. Figure 8 shows the influence of the distance l on v_a for $b = 20$ mm. It is observed from this figure that for $l = 10$ and 20 mm the velocity of the spreading crack v_a becomes, at some step of the crack propagation, equal to zero, which means that crack-arrest phenomena take place. In Fig. 9 the variation of the velocity of propagation of the short crack v_b vs the actual length L_a of the long crack is plotted. From this figure we conclude that v_b increases up to a certain length of the long crack L_a and then it diminishes becoming equal to zero, i.e. crack

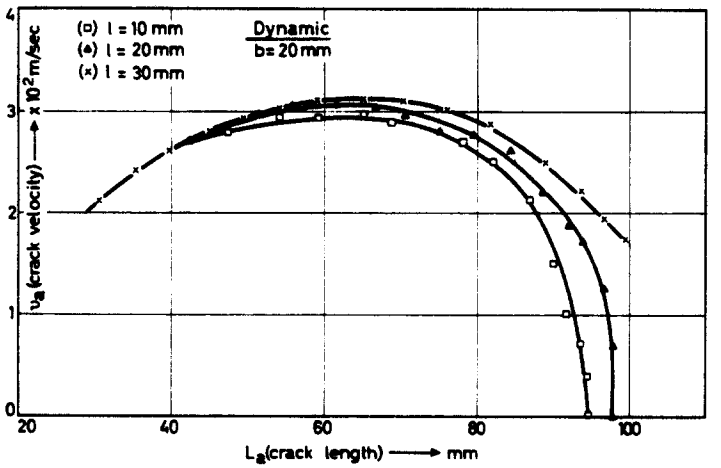

Fig. 8. Variation of the crack propagation velocity v_a of the larger crack in a double-cracked specimen vs the actual crack length L_a for a dynamic loading which causes the propagation of the smaller crack.

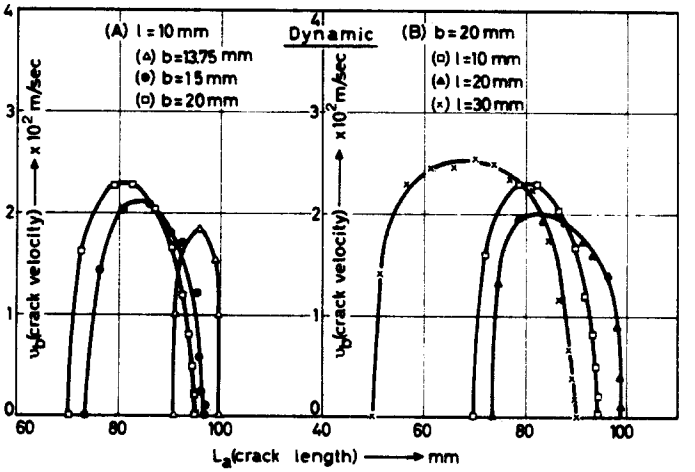

Fig. 9. Variation of the crack propagation velocity v_b of the smaller crack vs the actual crack length L_a of the greater crack for the case of Fig. 8.

arrest phenomena are also observed in the short crack. The crack arrest phenomenon which takes place on both cracks can also be observed from the six last photographs of Fig. 5, where it is apparent that both cracks are not propagating anymore although they are approaching either to the longitudinal boundary of the specimen (long crack), or the already propagated and overlapped long crack (short crack).

We can also state that, while the cracks are stationary, their caustics are increased, which means that an accumulation of elastic strain potential energy takes place at the crack tips, which is required for the further crack propagation. This accumulation of elastic strain energy for the shorter stationary crack is not sufficient to initiate again the spreading of this crack. However, after some time interval the longer crack always starts to propagate, whereas the smaller crack remains stationary. Figure 10 shows twelve successive photographs of the crack propagation procedure taken with a smaller frequency of the high-speed camera so that the whole phenomenon of crack propagation be better recorded. We can derive from this figure that at the time instant $t = 256\,\mu$sec the propagation of both cracks is stopped for a long period, during which the caustic at the tip of the longer crack increases, while the caustic at the tip of the smaller crack decreases. This means that a strain potential energy is accumulated at the tip of the longer crack and it increases until it reaches the critical value for crack propagation while the corresponding energy at the tip of the smaller crack diminishes. When the required energy reached its critical value, the longer crack starts to propagate following a new propagation path forming a corner point with the previous one. As the longer crack propagates, the potential

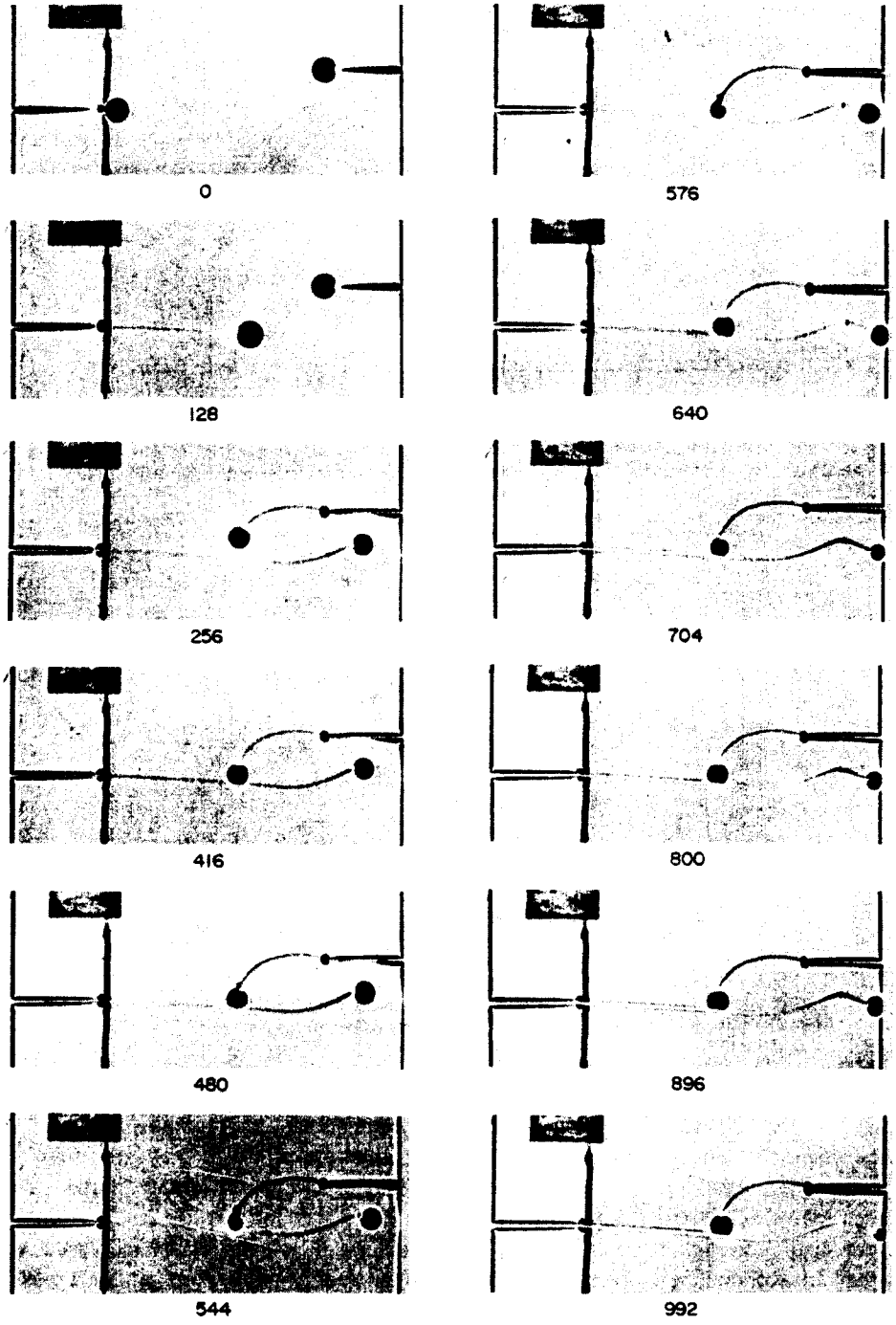

Fig. 10. Series of photographs obtained with a high-speed camera in a plexiglas specimen containing two skew-parallel edge cracks. It can be derived from this figure that while the first larger step of the crack propagation lasts 256 μsec, the second smaller step lasts 450 μsec, indicating significant crack arrest phenomena.

energy of the smaller crack increases; however it does not reach the required value for the propagation of this crack.

The intercrack distance l greatly influences the critical length L_{ac} of the longer crack for which the shorter crack starts to propagate. For the determination of the value of the distance l for which both cracks propagate, a series of experiments with $b = 20$ mm and l variable took place. From these experiments it was concluded that the most favourable values of the distance l, for which both cracks are propagated, are included in the interval $30\,\text{mm} < l < 35.5\,\text{mm}$.

Indeed, it was found that for $l = 10$, 20 and 25 mm the critical length L_{ac} was respectively $L_{ac} = 70$, 73.5 and 80 mm. For $l = 27.5$ mm the shorter crack remained stationary while for $l = 30$, 32.5 and 35 mm an early initiation of propagation of the shorter crack happened at a length $L_{ac} \simeq 50$ mm. For l higher than 37.5 mm again the crack b remained stationary. This peculiar phenomenon, showing that the dependence of the propagation of the smaller crack on the intercrack distance l is not continuous and it is strongly dependent on the geometrical configuration of the cracked plate will be studied in more detail in a subsequent publication.

Also the maximum value of the propagation velocity $v_{b\max}$ of the shorter crack depends on the value of the critical length L_{ac}. This is shown in Fig. 9(b), from which it is concluded that the propagation velocity v_b of the shorter crack increases with the time interval for which this crack starts to propagate. Thus, for $l = 30$ mm, for which the propagation of the shorter crack takes place at an early step of the propagation of the longer crack ($L_a = 50$ mm), the maximum value of the propagation velocity $v_{b\max}$ is 260 msec^{-1} whereas for $l = 20$ mm, for which the shorter crack propagates at a later step of the propagation of the longer crack ($L_a = 73.5$ msec^{-1}), we have $v_{b\max} = 200$ msec^{-1}.

Considering now the dependence of the maximum propagation velocity $v_{b\max}$ of the shorter crack for a constant value of the intercrack distance l on the value b of its length, we conclude that $v_{b\max}$ increases as b increases. This is shown in Fig. 9(a). From a series of tests it was also concluded that for $l = 10$ mm and $b < 13.75$ mm the shorter crack does not propagate. It is thus concluded that for a given intercrack distance l there is a critical value of the length b of the shorter crack, for which this crack propagates. As the value of length b increases beyond its critical value, the conditions for propagation of this crack become more favourable, i.e. this crack propagates at an early step of propagation of the longer crack. Thus, we derive that for $b = 13.75$, 15.00 and 20.00 mm this crack propagates when the actual length L_a of the longer crack takes the values $L_a = 90.5$, 73.5 and 70.0 mm respectively.

From the caustics created around the tips of both cracks the values of the corresponding stress intensity factors were determined by using relation (4). The constants entering this relation were evaluated experimentally for the particular batch of plates made of PMMA used in the tests and were found $c_t = 0.74$ m^{2}N^{-1}. Furthermore, the different distances in the elements of the experimental set-up used in these particular tests were $z_0 = 88$ cm, $z_i = 276$ cm, $\lambda = 0.758$. The value of the stress optical constant c_t found in these tests coincides with the value determined in Ref. [15] under similar experimental conditions as those in the present work. The values of the dynamic stress intensity factors obtained by using the method of caustics in the experiments made most probably differ from the corresponding theoretical static values. Because of the complicated geometry as the two cracks propagate and overlap and dynamic loading of the specimen, the true values of the dynamic stress intensity factor could not be evaluated so that a comparison between true-dynamic and static values of the stress intensity factors was not possible.

Figure 11 shows the variation of the stress intensity factors K_a and K_b at the tips of both cracks vs the actual length L_a of the larger crack for the quasi-static loading mode when $b = 20$ mm and $l = 10$, 20 and 30 mm. It may be derived from this figure that the influence of the intercrack distance l on the values of K_a and K_b is insignificant. In Fig. 12 the variation of K_a and K_b for a specimen with $b = 15$ mm and $l = 20$ and 30 mm loaded dynamically vs the actual length L_a of the larger crack is presented. For the configurations of cracks studied in this figure only the larger crack is propagated. It is shown from this figure that the value of the stress intensity factor K_b increases continuously. However, this factor remains small enough to cause a spreading of this crack. We can also deduce that K_b becomes larger for an intercrack distance $l = 30$ mm than for $l = 20$ mm, which means that the case when $l = 30$ mm is more favourable for the propagation of the shorter crack than the case when $l = 20$ mm.

In Figs. 13 and 14 the variations of the stress intensity factors K_a and K_b vs the actual length L_a of the larger crack for the dynamic loading mode when $b = 20$ mm and $l = 10$, 20 and 30 mm are presented. In all configurations of cracks corresponding to these figures both cracks are propagated. From Fig. 14 it can be derived that the values of K_b are high enough to cause the propagation of the smaller crack.

It can be further deduced from these figures that, while the variation of K_b was rather flat presenting a weak maximum during the initiation of propagation of this crack and a weak

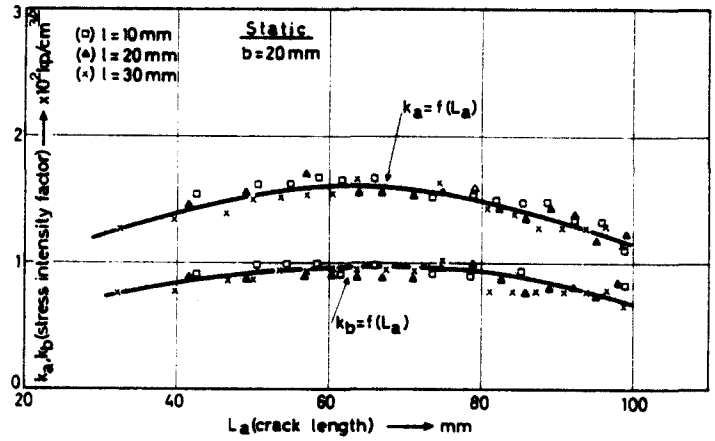

Fig. 11. Variations of the stress intensity factors K_a and K_b of the cracks vs the actual length L_a of the larger crack for a quasi-static loading.

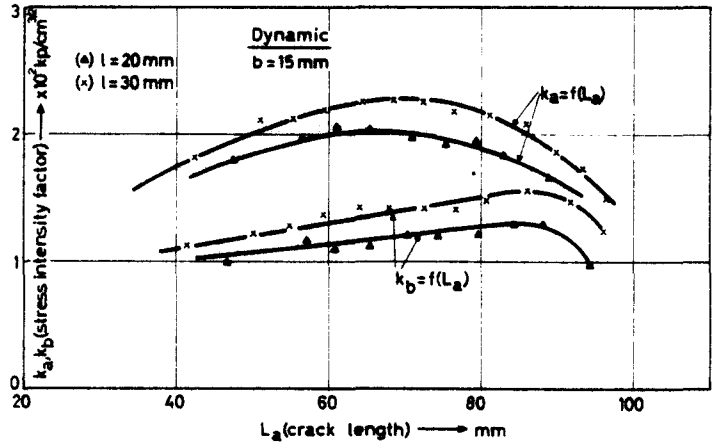

Fig. 12. As in Fig. 11 for a dynamic loading which does not cause the propagation of the smaller crack.

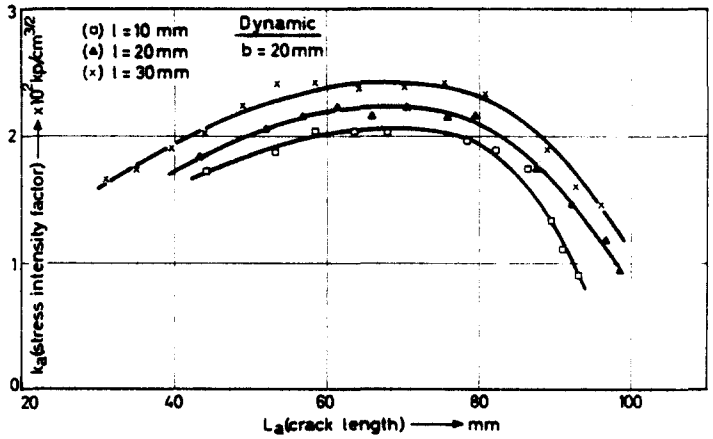

Fig. 13. Variation of the stress intensity factor K_a vs the actual crack length L_a for a dynamic loading which causes the propagation of both cracks.

reduction when the two moving cracks were overlapping each other, the variation of K_a for the longer and initially propagating crack was at the beginning of the process slowly increasing, then passing through a flat maximum and then steadily and rapidly decreasing. This maximum appeared when the crack was approaching the stationary and shorter crack and the decrease of K_a started when the two cracks overlap each other.

Furthermore, in Fig. 15 the value of the stress intensity factor K is presented as a function

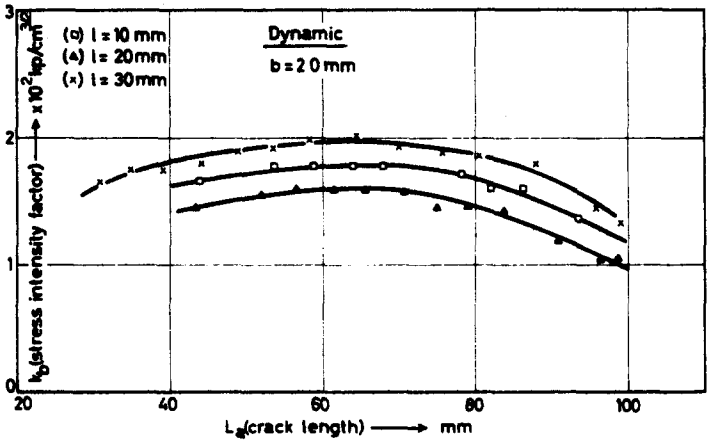

Fig. 14. As in Fig. 13 for the stress intensity factor K_b of the smaller crack.

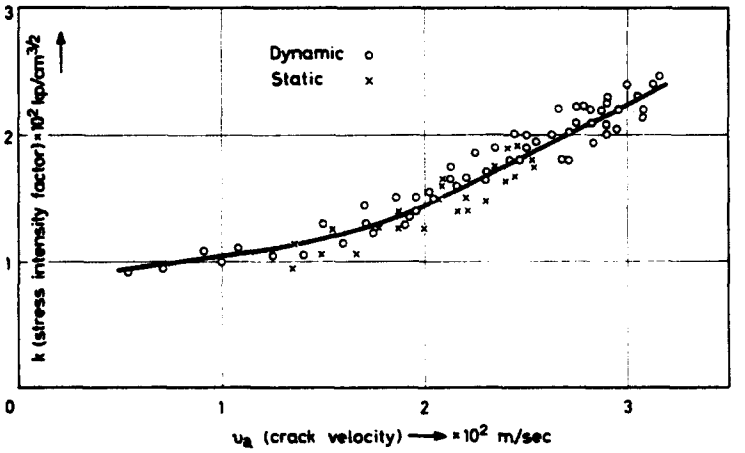

Fig. 15. Variation of the dynamic stress intensity factor K vs crack velocity v_a.

of the crack velocity v_a. The curve shown in this figure was obtained by using the previously mentioned results for the crack velocity and the stress intensity factor at crack tips for different crack lengths during the time interval when the cracks considered are propagated. Both cases of quasi-static and dynamic loading of the cracks have been considered in Fig. 15. Moreover, both types of cracks have been considered in this figure, from which it is realized that the dynamic stress intensity factor K at a crack tip during its propagation, which is a function of the crack length L, the applied load σ on the cracked specimen and time t is dependent only on the crack velocity v, that is

$$K(L, \sigma, t) = K_D(v). \tag{5}$$

Equation (5) holds satisfactorily, as can be seen from Fig. 15 and the function $K_D(v)$ is the dynamic fracture toughness of the material of the specimen. This function does not depend on the crack considered, or on the way that the load σ is applied, that is quasi-statically or dynamically.

Another important result, which may be derived from the caustic patterns of each individual test, concerns the mode of loading and the stress distribution at the crack tips as these cracks propagate. It has been previously found that the orientation of the longitudinal axis of the caustic relative to the actual axis of the crack at its tip is a measure for the evaluation of the complex stress intensity factor $K^* = K_I - iK_{II}$, where K_I is the opening mode and K_{II} the edge-sliding mode components of the complex value K^* of the stress intensity factor[16]. Indeed, the angle formed between the crack axis and the longitudinal axis of the caustic at each

instant is directly related to the ratio $\mu = K_{II}/K_I$. Based on this fact, we have examined all series of photographs for each individual test. As a general conclusion it may be stated that: (i) For crack geometries where the short crack remains stationary, K_{Ia} and K_{Ib} are operative while K_{IIb} remains always equal to zero. K_{IIa} is almost zero and in any case it takes only small values. (ii) For crack geometries where both cracks propagate, there is an interaction between the cracks when they approach each other and a deviation of their paths from their transverse orientations. However, although the angular displacements of both cracks toward the other crack are of the order of $\pi/4$ for the short crack and of $\pi/3$ for the large crack, the relative rotation of the corresponding caustics is only insignificant. This indicates that the stress field in the ligament between the two cracks, which is at least two-dimensional, has such orientations of the principal-stress trajectories near the crack tips, which are parallel and normal to the tangent at the crack tips and therefore shear is insignificant there. It is worthwhile mentioning that the higher distortion in the stress field exists at the longer crack, where the corresponding caustics are much more rotated than those corresponding to the tips of the short cracks. In general, the edge sliding-mode stress intensity factor K_{II} is very small during the propagation of the cracks. This can be derived from the fact that the axes of caustics are always almost coincident with the instantaneous axes of the propagating crack the angles between these two axes not exceeding in limiting cases the order of 10°. These cases appear especially when the cracks overlap and they are angularly displaced to become almost parallel to the direction of the applied load. This fact indicates that the stress field in the vicinity of the overlapped cracks is complicated. A dynamic photoelastic study of these fields is actually under progress to define the progressive variation of the field of the principal-stress trajectories when the cracks propagate. Nevertheless it seems probable that these very small values of K_{II} cause the cracks to turn to maximize K_I. A detailed study concentrated at the phase of propagation of cracks will enable us to estimate the values of K_{II} and to evaluate the influence of this factor on the angular displacement, decceleration and finally the arrest of the overlapping cracks. In any case, a thorough study of the stress fields in the ligaments between cracks made by photoelasticity may elucidate the mechanism of rotation of the propagating skew parallel cracks which is an important phenomenon appearing everywhere in branching of cracks.

One more interesting problem is to find the variation of the dynamic stress intensity factor during crack arrest if any. This cannot be easily determined by the experiments already made because of the fact that crack arrest takes place in a very short time interval. Nevertheless, it is believed that this problem will be investigated and reported in a subsequent paper.

CONCLUSIONS

In the present paper the behaviour of two skew-parallel and unequal edge cracks overlapping each other during their spreading through the plate in either a quasi-static or a dynamic tensile stress field was investigated. From this study the following conclusions can be derived:

(i) For the case of the quasi-static loading only the longer crack was propagated, while the short crack remained stationary.

(ii) For the case of the dynamic loading: (a) The propagation of both cracks depends on the geometrical configuration of the cracks in the plate. (b) The dependence of the propagation of the shorter crack on the value of the intercrack distance l is discontinuous. (c) The value of the maximum velocity of propagation of the shorter crack is inversely proportional to the actual length of the larger crack for which the propagation of the shorter crack starts. (d) The maximum velocities of propagation of the larger crack are larger than their corresponding values for the quasi-static loading mode. (e) The maximum crack-propagation velocities for both the quasi-static and the dynamic-loading modes are lower than the critical crack propagation velocity and the velocities obtained under purely dynamic loading.

(iii) For the quasi-static loading mode a large amount of inelastic deformation was observed, at the end of the initially propagated longer crack, while such phenomena were not observed for the dynamic loading mode.

(iv) The stress intensity factors at the tips of both cracks for the quasi-static modes were always smaller than the dynamic stress intensity factors.

(v) For the dynamic loading mode and for certain geometrical configurations of the cracked

specimens strong crack arrest phenomena were observed, resulting in large time intervals for the complete fracture.

(vi) Although the crack path during the crack propagation is curved, the amount of the introduced edge sliding-mode stress intensity factor at the crack tip was insignificant. However, this small amount of K_{II} caused rotations of the crack-axes for maximizing the respective K_I.

Acknowledgements—The author wishes to express his thanks to his collaborators Mrs. Leta Papadopoulou and Mr. Photis Katsamanis for their help during the execution of the experiments contained in this paper.

REFERENCES

1. H. Schardin and W. Struth, *Bruchvorgänge in Glas*. 2 *Techn. Phys.* **18**, 474 (1937).
2. F. Katsamanis, D. Raftopoulos and P. S. Theocaris, The dependence of crack velocity on the critical stress in fracture. *Exp. Mech.* **17**, 128 (1977).
3. B. K. Broberg, The propagation of a brittle crack. *Arkiv för Fysik* **18**, 159 (1960).
4. P. S. Theocaris and F. Katsamanis, Response of cracks to impact by caustics. *Engng Fract. Mech* **10**, 197 (1978).
5. A. S. Kobayashi, B. G. Wade and D. E. Maiden, Photoelastic investigation of the crack-arrest capability of a hole. *Exp. Mech.* **12**, 32 (1972).
6. K. Ishikawa, A. K. Green and P. L. Pratt, Interaction of a rapidly moving crack with a small hole in polymethylmethacrylate. *J. Strain Anal.* **9**, 233 (1974).
7. G. I. Barenblatt, The mathematical theory of equilibrium cracks in brittle fracture. *Adv. Appl. Mech.* **7**, 55 (1962).
8. E. Smith, The spread of plasticity between two cracks. *Int. J. Engng Sci.* **2**, 379 (1964).
9. T. Yokobori, M. Ichikawa and M. Ohashi, Interaction between elastic cracks, dislocation cracks and slip bands. *Proc. 1st Int. Conf. Fracture* **1**, 167 (1966).
10. P. S. Theocaris, The spread of plastic zones between symmetric edge cracks. *Israel J. Techn.* **8**, 367 (1970).
11. P. S. Theocaris, Interaction between collinear asymmetric cracks. *J. Strain Anal.* **7**, 186 (1972).
12. P. S. Theocaris, Interaction of cracks with other cracks or boundaries. *Int. J. Fract. Mech.* **8**, 37 (1972).
13. G. D. Gupta and F. Erdogan, The problem of edge cracks in an infinite strip. *J. Appl. Mech.* **41**, 1001 (1974).
14. P. S. Theocaris, Local yielding around a crack tip in plexiglas. *J. Appl. Mech.* **37**, 409 (1970).
15. D. D. Raftopoulos, D. Karapanos and P. S. Theocaris, Static and dynamic mechanical and optical behaviour of high polymers. *J. Phys. D (Appl. Phys.)* **9**, 869 (1976).
16. P. S. Theocaris and E. Gdoutos, An optical method for determining opening mode and edge-sliding mode stress intensity factors. *J. Appl. Mech.* **39**, 91 (1972).